Light scattering study of the glass transition in salol

D. L. Sidebottom and C. M. Sorensen
Department of Physics, Kansas State University, Manhattan, Kansas 66506
(Received 28 December 1988)

We have performed photon correlation spectroscopy experiments to measure the lifetimes of density fluctuations in liquid salol in both the normal and supercooled regimes down to its glass transition at −55 °C. Two modes were found to exist: a temperature-independent, hydrodynamic mode which we ascribed to entropy fluctuations and called the heat mode, and a strongly temperature-dependent, nonhydrodynamic mode due to internal, structural relaxations. We find that the internal relaxations suppress the heat mode when the heat-mode relaxation time is comparable to or less than the internal-mode relaxation time. This suppression occurs in the same temperature regime as a loss of power-law behavior for the viscosity as predicted by mode-coupling theory. We argue that the phenomena of the glass transition are a consequence of this suppression of the hydrodynamic heat mode by the internal relaxation mode as the temperature falls.

I. INTRODUCTION

It is well known that many liquids can be cooled below their equilibrium melting points and continuously solidified without crystallization to form glasses. It has been suggested that this glass transition is universal to all liquids if fast enough cooling rates could be achieved.[1] The approach to the glass is characterized by rapidly increasing viscosities and relaxation times as the system is cooled. The glass transition itself is marked by rounded discontinuities in the thermodynamic susceptibilities of the system. The glass transition temperature is not precisely fixed, however, since it is a function of the cooling rate. This latter fact is important in illustrating the kinetic nature of the glass transition.

The nature of the glass transition and associated phenomena have been the subject of numerous past investigations.[2] Recently, a new theoretical approach has been conceived which can be generally classified in terms of mode-coupling theories.[3–8] These theories predict a diverging viscosity, indicative of a glass transition, in relatively simple systems due to coupling of long-lived, short-length-scale density fluctuations to the viscosity. The earliest of these approaches involved first-order perturbation theory and predicted a power-law divergence in the viscosity

$$\eta=\eta_0(T-T_0)^{\mu}\ , \tag{1}$$

with $\mu\simeq -1.8$. It was suggested that the singular temperature could be identified with the glass transition temperature. Subsequent theoretical work has shown that (1) eventually fails near T_0.[6] Experimental work by Taborek, Kleiman, and Bishop[9] showed that Eq. (1) described very well the viscosity data for a number of liquids which were fragile glass formers according to Angell's classification scheme.[10] The fit with $\mu\simeq -2$ was better, in fact, than the usual Vogel-Tamman-Fulcher (VTF) equation, $\eta\sim\exp[A/(T-T_{\rm VTF})]$, when η was less than 10–1000 P, but failed for larger η. They also showed that the temperature T_0 was significant in that it divided the viscosity behavior into two regimes, one for which $T>T_0$ and Eq. (1) held and the other for which $T<T_0$ and an Arrhenius behavior described the viscosity. Hence, T_0 may carry more significance than the glass transition temperature, T_g, where the viscosity is uniformly Arrhenius, and which is experimental time-scale dependent. They concluded that if the mode-coupling transition has any physical significance it is distinct from the glass transition and probably occurs at a much higher temperature.

A key quantity in the mode-coupling theories, and in the theory of condensed matter in general, is the density-correlation function. It is nonlinear density fluctuations which lead to the mode-coupling prediction of the glass transition in hard-sphere systems.[5] Thus, it is a relevant task to study the behavior of the density fluctuations in a liquid as it approaches T_g. Light scattering probes long length and time scales of the density-correlation function. The spectrum of light scattered from a liquid shows a central elastic line, the Rayleigh line, flanked on each side by two Brillouin lines.[11] This central line can have two components which are relevant to our discussion. There is a heat-mode component in which density fluctuations are driven by entropy fluctuations. This mode is hydrodynamic and thus its relaxation time depends on the square of the scattering wave vector, q^2. There is also the so-called Mountain component which is not hydrodynamic, hence the relaxation time is independent of the wave vector (q^0), and is related to internal structural relaxations in the liquid.[11] A considerable amount of work has established that the Mountain component in a variety of supercooled liquids and glasses can be described by a broad distribution of relaxation times with an average relaxation time that scales roughly with η.

One group has paid attention to the interaction of the q^0 and q^2 modes of the spectrum. Allain-Demoulin *et al.*[12–15] have stressed the importance of the relative time scales of the heat and Mountain modes, τ_H and τ_M.

When $\tau_H > \tau_M$, the system behaves as a liquid, but when $\tau_M > \tau_H$ the heat modes disappear and the system behaves like a glass.

The behavior of the density fluctuation is important in the behavior of the thermodynamic susceptibilities. The discontinuity at T_g of, for example, the specific heat should be related to the freezing out of entropy fluctuations. While these thermodynamic discontinuities are ascribed to the freezing out of "configuration" degrees of freedom, an exact concept of the modes responsible has not yet been given.

In this paper we present a study of the two central modes of the light scattering spectrum of liquid salol for tempertures starting above the melting point and cooled through the regime of T_0, as determined from the viscosity, down to the glass transition temperature. Salol can be classified as a fragile glass[10] in that a plot of $\ln\eta/\eta_g$ versus T_g/T, where η_g is the viscosity at the glass transition, is distinctly curved and falls below Arrhenius or strong-glass behavior. The molecular structure of salol (phenyl salicilate) is sufficiently complex (two benzene rings connected via a carboxylic bridge) to allow for coupling to internal degrees of freedom which, as we shall see below, is an important quality for such molecular, fragile glasses. Like Allain-Demoulin *et al.* before us, we pay particular attention to the interplay of the hydrodynamic heat mode and the nonhydrodynamic Mountain mode due to internal structural relaxations. We find that the Mountain mode begins to have an effect on the spectrum of density fluctuations in the region of T_0, i.e., where deviations from Eq. (1) occur. We further support the contention of Taborek *et al.* that the significance of T_0 is different than that of T_g. T_g represents a temperature at which the internal relaxations seen in the Mountain mode become comparable to typical and somewhat arbitrary experiment times. On the other hand, we find T_0 divides the temperature range into a high-temperature, low-viscosity regime in which hydrodynamic fluctuations occur at all scales, and a low-temperature, large-viscosity regime in which the internal relaxations have destroyed the hydrodynamic fluctuations. Hence, the source of the glass transition, we will contend, lies not in the mode-coupling theory prediction of a singularity at T_0, but rather in the concept that the nonhydrodynamic, internal relaxation modes remove hydrodynamic degrees of freedom at progressively larger length and time scales until these scales become macroscopic.

II. EXPERIMENTAL METHOD

A. Set up

The salol (phenyl salicilate) used in this study was purchased from Aldrich Chemical and was assayed by Aldrich as 99% pure. Due to its substantial hydroscopic nature, it was necessary to dehydrate the salol. Early light scattering results revealed the formation of ice crystals at around 0 °C. Molecular sieves (4 Å) were tried as a desiccant, but caused a noticeable red discoloration of the salol. The desiccant $CaCl_2$, however, produced no discoloration. Batches of salol were dried over $CaCl_2$ with occasional stirring in an oven at 50 °C ($T_{\text{melt}} = 46$ °C) for no less than three days.

Photon correlation spectroscopy[16] was used to measure the relaxation of density fluctuations which cause the central, quasielastically scattered modes of the light scattering spectrum in salol. These measurements were made over the temperature range −60 °C to +70 °C. Measurement of the hydrodynamic modes of salol required small scattering angles to increase the heat-mode time to values large enough for our correlator to measure ($> 10^{-5}$ sec). The scattering angles chosen were $1.1° \pm 0.1°$ and $2.3° \pm 0.1°$.

The greatest difficulty experienced in producing samples capable of small-angle light scattering necessary for our measurements was the elimination of small particles present in the melt. Due to the high viscosity of salol just above the melting point, it was necessary to use a pressurized filtration bomb which could be heated to about 60 °C. Salol was then filtered through a 0.22 μm millipore Teflon filter into the scattering cell.

Although significantly improved, initial samples produced in this manner often still possessed a large number of particles. We discovered that these particles were produced after filtration when the salol dislodged more particulates from the interior of the scattering cell. By repeated rising of the cells with freshly filtered salol, samples were produced which, although they still contained a few particles, were acceptable for our light scattering purposes.

To conduct scattering at such small angles it is imperative to remove as much of the stray light as possible. A major source of such undesirable light was due to scattering from the air-glass interface of the scattering cell. Removal of these "wall spots" was accomplished by separating the entrance and exit windows by a long path length cell. Our small-angle scattering cell consisted of an 8 cm long section of 14 mm i.d. glass tube terminated at flat ends by optical grade (polished) windows. An additional tube was attached at the midsection to allow the cell to be filled.

Even with the above precautions, there was sufficient stray light to produce weak signal-to-background and heterodyne correlation spectra.

Below −25 °C, the q-independent Mountain mode becomes dominant and was most easily studied at $\theta = 90°$. For this scattering geometry, a conventional 1 cm^2 glass cell was employed. At 90°, the stray light scattered from elusive particles and from the cell walls was negligible, and a strong signal-to-background ratio assured us that homodyne spectra were obtained. Comparison of Mountain-mode data taken at 2.3° with those taken at 90° verified the respective heterodyne and homodyne nature of the detection.

Our optical arrangement consisted of an Ar^+ laser emitting at the 4880 Å wave length. This light was focused by a lens to about 100 μm diameter beam waist as it passed through the center of the scattering cell. The scattered light was collected by a lens and the scattering volume was imaged onto a slit-pinhole arrangement located about 50 cm ahead of the cathode of a photomultipler tube (PMT). This arrangement provided sufficient

special coherence of the light impinging upon the cathode to produce an acceptable signal-to-noise ratio and allowed for easy blockage of the wall spots. The PMT output was amplified, digitized, and fed to a commercial correlator which computed the correlation function.

In order to characterize the Mountain mode, which is typically described by a stretched exponential, several sets of correlation data at different sample times covering a number of decades in time were overlayed to obtain the complete correlation function. This required calculation of the background level of the correlation function from the photocount statistics so that the different spectra could be properly normalized before they were merged.

Temperature control was achieved by placing the samples in thermal contact with metal holders cooled by circulated bath fluids. A thermistor and bridge circuit was used to determine the temperature of the metal holders which was accurate to $\pm 0.1\,^{\circ}\mathrm{C}$.

B. Analysis

The structure factor $S(q,t)$ is displayed in Fig. 1 for selected temperatures ranging from $+40\,^{\circ}\mathrm{C}$ to $-30\,^{\circ}\mathrm{C}$. The spectra in Fig. 1 were collected at a scattering angle of $\theta = 1.1^{\circ}$ and those at 2.3° show qualitatively similar behavior. For all temperatures above about $-20\,^{\circ}\mathrm{C}$ only a single exponential relaxation was found, which was q^2

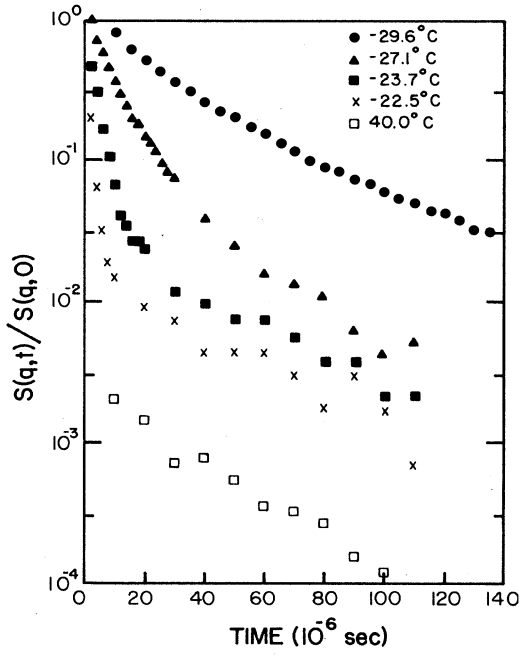

FIG. 1. The dynamic structure factor for a range of temperatures which overlap the crossover regime $\langle \tau \rangle \simeq \tau_H$. The appearance of the Mountain mode is clearly discerned at $-22.5\,^{\circ}\mathrm{C}$ as the shorter decay. The heat mode is still apparent at $-27.1\,^{\circ}\mathrm{C}$. $\theta = 1.1^{\circ}$. For clarity the lower three data sets have been multiplied as follows: □, 2×10^{-3}; ×, 2×10^{-1}; ■, 5×10^{-1}.

dependent and whose temperature dependence was weak. These relaxations are the hydrodynamic heat mode.

In the temperature range between $-20\,^{\circ}\mathrm{C}$ and $-30\,^{\circ}\mathrm{C}$, the spectra displayed two distinct relaxations. The first relaxation which comprises the tail of the spectrum at $-22.5\,^{\circ}\mathrm{C}$ appears to be a remnant of the heat mode observed at higher temperatures. The other relaxation grows rapidly in both magnitude and time with decreasing temperature. This second relaxation is the Mountain mode associated with structural relaxations. We have also observed it in the depolarized light scattering which we do not report here.

Below about $-30\,^{\circ}\mathrm{C}$, the heat mode can no longer be distinguished in the spectrum. The inability to measure this mode is due to the relative strength of the Mountain mode. The signal-to-background ratio of the scattered light due to the Mountain mode is roughly 1 order of magnitude larger than that of the disappearing heat mode.

The exponential heat-mode structure factor part of the spectrum was fit to a two-cumulant fit

$$S_H(q,t) = B + Ae^{-\mu_1 t + \mu_2 t^2/2} . \tag{2}$$

In Eq. (2), B is the background determined either from the time-delayed last eight channels of the correlation spectrum or calculated from the photocount statistics. A is a signal amplitude. The cumulants are μ_1 and μ_2 and the ratio μ_2/μ_1^2 was always found to be small ($\lesssim 0.05$) indicating the expected exponentiality. The first cumulant is the key quantity

$$\mu_1^{-1} = \tau_H = (2D_T q^2)^{-1} . \tag{3}$$

τ_H is the heat-mode relaxation time, D_T is the thermal diffusivity, and q is the scattering wave vector with magnitude

$$q = \frac{4\pi n}{\lambda}\sin(\theta/2) . \tag{4}$$

Here λ is the optical wavelength and n is the medium refractive index.

The values of τ_H are shown in Fig. 2 for both $\theta = 1.1^{\circ}$ and 2.3°. At the highest temperature τ_H displays the expected q^2 dependence although as the temperature is lowered into the regime where both modes are present this behavior declines. This is qualitatively similar to the results of Allain and Lallemand.[14]

As shown in Fig. 1, the Mountain mode begins to appear below about $-20\,^{\circ}\mathrm{C}$. In the region $-20\,^{\circ}\mathrm{C} > T > -30\,^{\circ}\mathrm{C}$ both modes are present and their characteristic relaxation times could be determined, although with limited accuracy. Since the Mountain relaxation is not hydrodynamic, i.e., it has no q dependence, once it appeared, we could obtain data for it at the experimentally easier 90° scattering angle.

As discussed above, the highly nonexponential nature of the Mountain relaxation required us to take data at a few to several different samples times and then combine these separate runs to create a complete $S_M(q,t)$. An example of this is shown in Fig. 3 for $T = -44.9\,^{\circ}\mathrm{C}$. One can see the relaxation spans more than three decades.

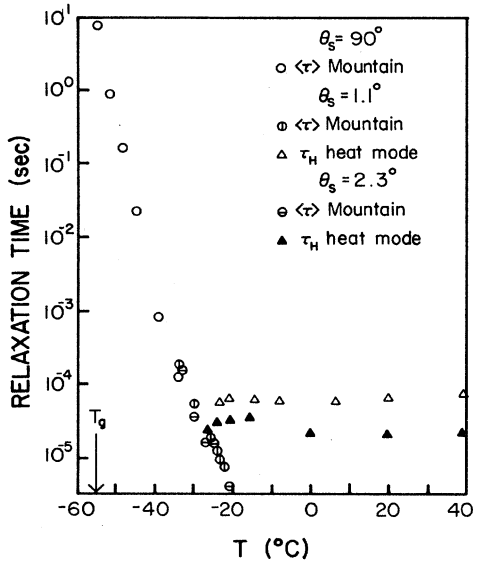

FIG. 2. The characteristic relaxation time of both the internal relaxation mode $\langle\tau\rangle$ and the heat mode τ_H vs temperature for liquid salol. The experimental glass transition temperature, $T_g=-55\,^{\circ}\mathrm{C}$ is indicated by the arrow.

The homodyne data taken at 90° were fit to a "stretched exponential" (or Kohlrausch) form

$$S_M(q,t)=Ae^{-2(t/\tau_M)^{\beta}}. \tag{5}$$

[Since the Mountain mode is q independent, the "q" in Eq. (5) is superfluous, but we keep it for consistent notation.] In Eq. (5) τ_M is a relaxation time and β describes the degree of nonexponentiality. The stretched exponential is due to a characteristic distribution of exponential relaxations with an average structural relaxation time given by[17]

$$\langle\tau\rangle=\tau_M\beta^{-1}\Gamma(\beta^{-1}). \tag{6}$$

Values of $\langle\tau\rangle$ and β obtained at $\theta=90°$ are given in Table I. The data obtained at 1.1° and 2.3° were less precise

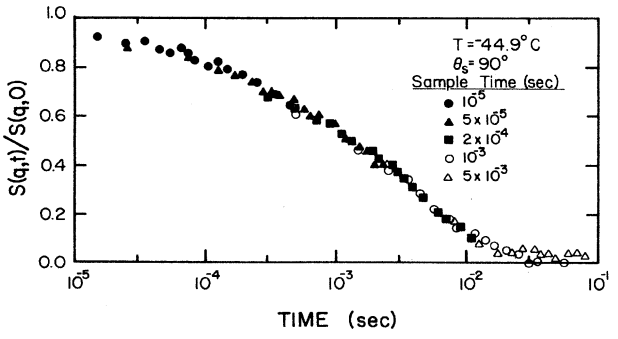

FIG. 3. The dynamic structure factor for the Mountain mode at −44.9 °C. This data is formed from the combination of five separate correlation functions and displays the highly nonexponential character of this mode.

TABLE I. Fit parameters to Eq. (5) for the Mountain mode and the average structural relaxation time at various temperatures.

T (°C)	τ_M (sec)	β	$\langle\tau\rangle$ (sec)
−33.5	8.1×10^{-5}	0.63±0.05	1.2×10^{-4}
−39.3	5.6×10^{-4}	0.61±0.05	8.3×10^{-4}
−44.9	1.2×10^{-2}	0.51±0.03	2.2×10^{-2}
−48.3	9.0×10^{-2}	0.51±0.03	1.6×10^{-1}
−51.5	6.1×10^{-1}	0.62±0.06	8.8×10^{-1}
−54.7	5.4×10^{0}	0.60±0.08	8.0×10^{0}

and also heterodyne data. Values of τ_M at these two smaller angles could be obtained [from Eq. (4) without the factor 2], and $\langle\tau\rangle$ estimated by assuming $\beta=0.6$, an average value implied by the 90° data. All these $\langle\tau\rangle$ data are included in Fig. 2 and are seen to be consistent.

III. RESULTS AND DISCUSSION

Figure 2 is our general result showing the relative temperature dependencies of the hydrodynamic, heat-mode relaxation times, τ_H, and the nonhydrodynamic, internal relaxation mode time, $\langle\tau\rangle$. The heat mode shows essentially no temperature dependence, whereas the internal relaxations show a very strong increase with decreasing temperature.

We believe Fig. 2 tells a potent story. τ_H is the characteristic relaxation time of hydrodynamic entropy fluctuations of wave vector q, hence length scale q^{-1}. As the internal relaxation time increases to the point where $\langle\tau\rangle\simeq\tau_H(q)$, the particular heat mode of wave vector q gets destroyed. This destruction is evident in Fig. 1 and in the work of Allain and Lallemand[14] who showed the intensity of the heat mode dropped by an order of magnitude at this point. Thus we have a picture wherein $\langle\tau\rangle$ sets a time scale. All $\tau_H(q)<\langle\tau\rangle$ are no longer operational, i.e., short-time- and short-length-scale heat modes have been destroyed, whereas all $\tau_H(q)>\langle\tau\rangle$ are still active in the relaxation spectrum of the liquid.

At what temperatures does this destruction of hydrodynamic modes occur? In Fig. 4 we plot the viscosity of salol[18,19] as a function of temperature in the manner of Taborek, Kleiman, and Bishop,[9] $\eta^{-1/2}$ versus T. The graph is linear at high T indicating Eq. (1) holds with $\mu=-2$. Extrapolation of this linear part to $\eta^{-1/2}=0$ yields a $T_0\simeq-10\,^{\circ}\mathrm{C}$. This is near the temperature range where the internal relaxation began consuming the hydrodynamic relaxation in our experiment (Fig. 2).

Of course there is nothing special about our particular experimental time scales and we should consider other time and length scales. Thus, in Fig. 5 we combine our data with Brillouin scattering results for $\langle\tau\rangle$ of Enright and Stoicheff.[19] The ranges of the two sets of $\langle\tau\rangle$ do not overlap but simple extrapolation suggests they are consistent. Now we observe from Fig. 4 that the viscosity's linear behavior, which indicates the power-law behavior of Eq. (1), begins to fail at ~280 K. From Fig. 5 this corresponds to $\langle\tau\rangle\sim10^{-9}$ to 10^{-10} sec. From extrapolation of our measured τ_H in Fig. 2, this corresponds to a

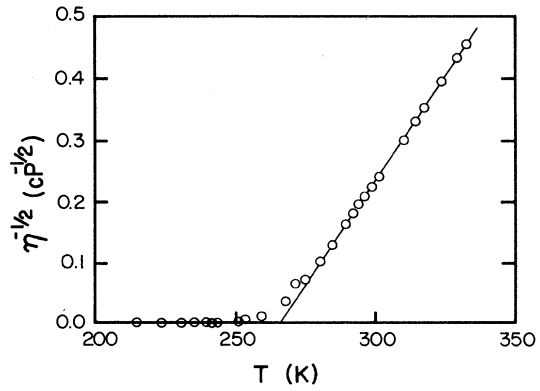

FIG. 4. $\eta^{-1/2}$ vs T for salol. Linear portion of graph indicates a good fit to Eq. (1) with $\mu=-2.0$ and $T_0=263$ K.

$q \simeq 10^{-2}$ Å^{-1}, i.e., a length scale of $q^{-1} \simeq 100$ Å. Thus it seems that the hydrodynamic, mode-coupling theory prediction of a power-law viscosity dependence, Eq. (1), begins to fail when microscopically short–time- and short–length-scale hydrodynamic fluctuations begin to be destroyed by the internal relaxations.

This match to "microscopically short" is not perfect. It seems to us on a qualitative basis that the fastest and smallest modes in salol might be more on the order of $\tau_H \sim 10^{-11}$ sec and $q^{-1} \sim 10$ Å. $\langle\tau\rangle$ is not changing very quickly in the region of $T=280$ K so perhaps the hydrodynamic modes are not being consumed very quickly and deviations from Eq. (1) are initially small.

To pursue these ideas further, we expect a liquid to behave like a liquid when it has hydrodynamic modes which can be excited. In fluid flow the viscosity follows liquidlike behavior as long as there is a full spectrum, time and length scale, of hydrodynamic modes available to the system. Liquidlike behavior could be the power-law behavior of the viscosity, Eq. (1). This is supported

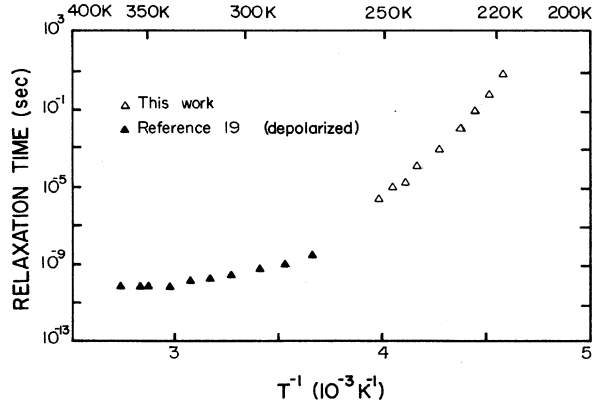

FIG. 5. Arrhenius plot of the internal relaxation mode time $\langle\tau\rangle$ in liquid salol. The high-temperature data were obtained by Enright and Stoicheff (Ref. 19) from the linewidth of the depolarized central peak.

by the lowest-order mode-coupling theories and the empirical results of Taborek *et al.*[9] who correlated the power-law coefficient to critical point viscosities. As the temperature falls, the internal relaxations kill the shortest–time- and shortest–length-scale hydrodynamic relaxations and deviations from the power law begin. Das and Mazenko[6] have written that nonhydrodynamic corrections cut off the power-law behavior, i.e., that freezing of fluctuations occurs first at small length scales; then hydrodynamics is pushed out to longer and longer length and time scales as temperature falls. We believe our data show this explicitly as deviations from the power law increases as nonhydrodynamic internal relaxations destroy the hydrodynamic heat modes.

The glass transition has long been viewed as a transition in which kinetics can freeze out thermodynamic pathways. This idea was expressed very well in the context of light scattering by Allain-Demoulin *et al.*[12,14] who essentially wrote that the glass transition is dependent on relative time scales: a liquid displays liquidlike light scattering spectra when the internal relaxation modes are short compared to the heat mode, and it displays glasslike scattering spectra when the internal modes are long compared to the heat mode.

This idea can, of course, be applied to phenomena other than light scattering. Recently Jackle[20] and Bengtzelius and Sjogren[21] have related the smooth jump discontinuities of the thermodynamic susceptibilities (ΔC_p, ΔK_T, and $\Delta\alpha$) to freezing out of density fluctuations. In our data we see this process at work. As an example, it is well known that the jump in the specific heat, which is usually used to define the glass transition temperature T_g, is cooling rate dependent. Recently, the method of specific-heat spectroscopy has increased by orders of magnitude the effective range of heating and cooling rates.[22,23] These results may be interpreted to show that the frequency dependent specific heat $C_p(\nu)$ has a liquid value when $\nu^{-1} > \langle\tau\rangle$ and a glass value when $\nu^{-1} < \langle\tau\rangle$. Recalling that the heat modes detected in light scattering are due to entropy fluctuations δS and that $C_p \sim \langle\delta S^2\rangle$, it follows that a liquid value of C_p can only be obtained when heat modes of the proper time scale still exist. This is when $\tau_H > \langle\tau\rangle$. Thus if $\nu^{-1} = \tau_H > \langle\tau\rangle$, the liquid value of C_p will be obtained.

We now wish to elaborate on the contention of Taborek *et al.*[9] that the mode coupling theories and the temperature T_0 have physical significance distinct from the glass transition. Our data show that T_0 is the temperature where the viscosity *would have diverged* if not for the glass transition. That is, destruction of hydrodynamic modes by internal relaxation modes destroys a hydrodynamic divergence of the viscosity.

On the other hand, the internal relaxation modes do not become significant until $\eta \sim 10$–1000 P. This large viscosity is due to the hydrodynamic modes. Thus, it is the hydrodynamic modes which seem to establish the proper conditions to set the nonhydrodynamic modes to work; they sow the seed of their own destruction. The nonhydrodynamic modes lengthen in time scale until they become comparable to experimental time scales and we then call this the "glass transition." Thus, the physi-

cal significance of the mode-coupling theories and T_0 may both stand apart from, and yet be tied to the glass transition.

Finally, we point out that salol is an example of a fragile glass former.[10] Strong glasses have very small thermodynamic discontinuities and do not fit the power law in Eq. (1) well. Hence our conclusions at this time apply only to fragile glasses. It is noteworthy, however, that strong glasses are microscopically well connected and hence internal relaxations may dominate even at high temperatures.

IV. CONCLUSIONS

Our measurements of the two central modes of the light scattering spectrum of supercooled liquid salol show that the nonhydrodynamic mode due to internal, structural relaxations in the liquid destroys the hydrodynamic mode due to entropy fluctuations when their time scales become comparable. That is, hydrodynamic entropy fluctuations are strongly suppressed for time scales (and corresponding length scales) shorter than the internal relaxation time. This suppression occurs in the same temperature regime that the viscosity deviates from power-law behavior as predicted by mode-coupling theories. We, therefore, have interpreted our data to indicate that the glass transition is a broad transitional process wherein hydrodynamic fluctuations get consumed at ever increasing time and length scales as the temperature falls. It is the loss of these hydrodynamic degrees of freedom which causes the characteristic thermodynamic discontinuities observed at the glass transition as well as the deviation from power-law behavior for the viscosity. Manifestation of the glass transition at a given time scale, such as a common laboratory time scale, is relatively sharp compared to the whole process because the internal relaxation time is strongly temperature dependent.

ACKNOWLEDGMENTS

This work was supported by National Science Foundation (NSF) Grant No. CHE-86-18576.

[1]D. Turnbull, Contemp. Phys. **10**, 473 (1969).
[2]For reviews, see J. Jackle, Rep. Prog. Phys. **49**, 171 (1986); M. I. Klinger, Phys. Rep. **165**, 275 (1988).
[3]E. Leutheusser, Phys. Rev. A **29**, 2765 (1984).
[4]U. Bengtzelius, W. Gotze, and A. Sjolander, J. Phys. C **17**, 5915 (1984).
[5]S. P. Das, G. F. Mazenko, S. Ramaswamy, and J. J. Toner, Phys. Rev. Lett. **54**, 118 (1985).
[6]S. P. Das and G. F. Mazenko, Phys. Rev. A **34**, 2265 (1986).
[7]T. R. Kirkpatrick, Phys. Rev. A **31**, 939 (1985).
[8]L. Sjogren and W. Gotze, J. Phys. C **20**, 879 (1987).
[9]P. Taborek, R. N. Kleimann, and D. J. Bishop, Phys. Rev. B **34**, 1835 (1986).
[10]C. A. Angell, in *Relaxation in Complex Systems,* Proceedings of the Workshop on Relaxation Processes, Blacksburg, Virginia, 1983, edited by K. Ngai and G. B. Smith (National Technical Information Service, U.S. Dept. of Commerce, Washington, DC, 1985), p. 3.
[11]R. D. Mountain, Rev. Mod. Phys. **38**, 205 (1966); J. Res. Nat. Bur. Stand. Sect. A **70**, 207 (1966); **72**, 95 (1968).
[12]C. Demoulin, C. J. Montrose, and N. Ostrowsky, Phys. Rev. A **9**, 1740 (1974).
[13]C. Allain-Demoulin, P. Lallemand, and N. Ostrowsky, Mol. Phys. **31**, 581 (1976).
[14]C. Allain and P. Lallemand, J. Phys. (Paris) **40**, 693 (1979).
[15]C. Allain, M. Berard, and P. Lallemand, Mol. Phys. **41**, 429 (1980).
[16]B. J. Berne and R. Pecora, *Dynamic Light Scattering* (Wiley-Interscience, New York, 1976).
[17]G. Fytas, C. H. Wang, D. Lilge, and T. Dorfmuller, J. Chem. Phys. **75**, 4247 (1981).
[18]W. T. Laughlin and D. R. Uhlmann, J. Phys. Chem. **76**, 2319 (1972).
[19]G. D. Enright and B. P. Stoicheff, J. Chem. Phys. **64**, 3660 (1976).
[20]J. Jackle, J. Chem. Phys. **79**, 4463 (1983).
[21]U. Bengtzelius and L. Sjogren, J. Chem. Phys. **84**, 1744 (1986).
[22]N. O. Birge and S. R. Nagel, Phys. Rev. Lett. **54**, 2674 (1985).
[23]P. K. Dixon and S. R. Nagel, Phys. Rev. Lett. **61**, 341 (1988).